Published in final edited form as:
Neuroscience. 2011 July 28; 187: . doi:10.1016/j.neuroscience.2011.03.055.

HIPPOCAMPAL INPUTS MEDIATE THETA-RELATED PLASTICITY IN ANTERIOR THALAMUS

M. TSANOV[a,b], **N. WRIGHT**[c], **S. D. VANN**[c], **J. T. ERICHSEN**[d], **J. P. AGGLETON**[c], and **S. M. O'MARA**[a,b,*]

[a]Trinity College Institute of Neuroscience, Trinity College Dublin, Ireland [b]School of Psychology, Trinity College Dublin, Ireland [c]School of Psychology, Cardiff University, UK [d]School of Optometry and Vision Sciences, Cardiff University, UK

Abstract

Hippocampally-driven oscillatory activity at theta frequency is found in the diencephalon, but an understanding of the fundamental role of theta in the hippocampo-diencephalic circuit remains elusive. An important strategy in determining how activity modifies oscillatory properties of hippocampo-diencephalic circuitry comprises investigations of anterior thalamic responses to their main inputs: the descending dorsal fornix and the ascending mammillothalamic tract. Here, we show that the amplitude of thalamic theta spectral power selectively increases after plasticity-inducing stimulation of the dorsal fornix, but not of the mammillothalamic tract in urethane-anaesthetized young male rats. Furthermore, we show that low-frequency stimulation (LFS) significantly augments the fornix-driven theta ratio (theta over delta power, T-ratio), in parallel with depressing thalamic synaptic responses. However, the mammillothalamic synaptic response after LFS did not correlate with the slow band of theta oscillation (low T-ratio), but did correlate positively with the fast band of theta oscillation (high T-ratio). Our data demonstrate that the descending direct fornix projection is a pathway that modulates theta rhythm in the hippocampo-diencephalic circuit, resulting in dynamic augmentation of thalamic neuronal responsiveness. These findings suggest that hippocampal theta differentially affects synaptic integration in the different structures with which the hippocampus is reciprocally connected.

Keywords

anterior thalamic nuclei; fornix; mammillothalamic tract; synaptic plasticity; theta oscillation; LTP

The functioning of the thalamus and the hippocampus cannot be fully elucidated without considering them as a unified network (Steriade, 2001; Warburton et al., 2001). In this context, hippocampal oscillations would be expected to have an impact on the neuronal activity of the anterior thalamic nuclei (ATN) but how the signals are actually processed through the hippocampo-diencephalic loop remains poorly understood. Large neuronal populations in ATN oscillate with frequency of 6–11 Hz, in the range of theta rhythm (Vertes et al., 2001; Tsanov et al., 2011a). Theta oscillations are a characteristic feature also of the main regions providing anterior thalamic inputs: the hippocampal formation and the medial mammillary bodies, that is the "medial" hippocampo-diencephalic system (Aggleton et al., 2010).

*Correspondence to: S. M. O'Mara, Trinity College Institute of Neuroscience, Trinity College Dublin, Dublin 2, Ireland. Tel: +353-1-896-8447; fax: +353-1-896-3183. smomara@tcd.ie. .

Europe PMC Funders Author Manuscripts

Theta rhythm has been especially related to the processes of episodic memory formation in the extended hippocampal system (Buzsáki, 2005). The hippocampus receives two main types of input: the first one is the theta input from the medial septum, which reverberates through hippocampo-diencephalic loop (Fig. 1A). The second hippocampal input is a highly-processed sensory information originating from multiple neocortical regions. The temporal convergence of activity from neocortical and diencephalic inputs would result in long-term storage of the encoded information. Because theta activity induces a fluctuation in cellular excitability, the probability that spatially-distant and otherwise non-interacting neurons discharge nearly simultaneously is substantially increased (Alonso and Llinas, 1989; Leung and Yim, 1991; Ylinen et al., 1995; Linden, 1999). A functional consequence of such oscillations is the modification of synaptic weights across distant neuronal populations (Buzsáki, 2002). Concurrently, brain regions that synchronize their theta rhythm with hippocampal activity would facilitate the strengthening of memory traces. Such theta synchronization has been observed between hippocampal and amygdala during fear conditioning (Seidenbecher et al., 2003), between hippocampus and visual cortex in response to visuospatial information (Tsanov and Manahan-Vaughan, 2009) and between hippocampus and cerebellum in response to external stimuli (Hoffmann and Berry, 2009; Wikgren et al., 2010). The connection between oscillatory patterns and hippocampal plasticity has been explored (Mehta et al., 2002; Dragoi et al., 2003; Hyman et al., 2003; Hasselmo, 2005), but very little is known about the activity-induced plastic changes in thalamus and their possible relations to theta rhythm processing.

The anterior thalamic nuclei appear to be vital for human episodic memory (Aggleton and Sahgal, 1993; Harding et al., 2000; Gold and Squire, 2006), while animal lesion experiments (including cross-disconnection studies) confirm the critical role of these nuclei for hippocampal-dependent learning (Parker and Gaffan, 1997; Warburton et al., 2001). Lesion studies in the hippocampus, fornix, and anterior thalamus in rats disrupt tests of temporal order discrimination (Fortin et al., 2002; Wolff et al., 2006). Crossed-lesion disconnection studies show that the hippocampus and anterior thalamic nuclei depend on each other for effective spatial learning (Warburton et al., 2000, 2001; Henry et al., 2004). Lesion studies in monkeys suggest that the fornix, mammillary bodies, and anterior thalamic nuclei function together in the learning of visual discriminations that are aided by contextual information (Parker and Gaffan, 1997). The link between episodic memory and theta rhythm raises an important question about the role of diencephalon and its major afferents—the fornix and the mammillothalamic tract in memory formation.

One intriguing proposal is that hippocampal theta, proceeding to ATN through direct fornical projections, sets thalamic neuronal responsiveness to stimuli coming from the ventral tegmental nuclei of Gudden via the medial mammillary bodies. The first step in exploring this hypothesis is to compare the effect of fornix and mammillothalamic fiber activation on thalamic theta oscillation, an issue addressed in this paper. Theta rhythm can be subdivided into two types: the first is dependent on motor activity and falls within a range of 8–12 Hz (high theta), while the second type consists of a slightly lower frequency (4–8 Hz, slow theta) and is dependent on the release of acetylcholine into the hippocampus from the septum (Bland et al., 1984; Bland, 1986; Sainsbury et al., 1987). The medial septum is commonly accepted as the pacemaker of theta in the limbic system (Brazhnik and Vinogradova, 1986), and inactivation of medial septum abolishes theta rhythmic discharge in hippocampus and mammillary bodies (Kirk et al., 1996). The hippocampus and mammillary bodies provide major monosynaptic inputs to the anterior thalamus, forming the “extended hippocampal system” (Vann and Aggleton, 2004). Thus, an important challenge is to determine if the activation of either of these inputs influences theta properties within the ATN. Of particular interest here is the comparison of the plasticity effects evoked after stimulation of the two major ATN inputs: the descending hippocampo-thalamic projection

Europe PMC Funders Author Manuscripts

and the ascending mammillothalamic tract. Of these pathways, we found that the fornix is a pathway that controls ATN theta amplitude, suggesting that hippocampus provides modulatory input to subcortical theta processing. Our data reveal hippocampal conditioning of thalamic theta, and reinforce the putative role of cortico-thalamic loops involved in episodic memory.

EXPERIMENTAL PROCEDURES

Animals

Experiments were conducted in accordance with European Community directive, 86/609/EC, and the Cruelty to Animals Act, 1876, and followed Bioresources Ethics Committee, Trinity College, Dublin, Ireland, and international guidelines of good practice. Male 7–10-week-old Lister-Hooded rats (Harlan, UK) were triple housed and maintained on 12/12 h light/dark cycles with food and water provided *ad libitum*.

Anterograde labelling, general surgical procedures

All animals were anesthetized with 6% sodium pentobarbital (Sigma-Aldrich, Gillingham, UK). Animals were then placed in a stereotaxic frame (Kopf, Tujunga, CA, USA) and small openings were made in the skull and dura to allow access for the 0.5 μl Hamilton syringes (Hamilton, Bonaduz, Switzerland), containing either wheat germ agglutinin (WGA, Vector Laboratories, Peterborough, UK) or wheat germ agglutinin conjugated to horseradish peroxidase (WGA-HRP, Vector Laboratories). After surgery, animals received a 5 ml subcutaneous injection of 5% glucose in 0.9% saline (Baxter Healthcare Ltd., Norfolk, UK), and Aureomycin antibiotic powder (Fort Dodge Animal Health Ltd, Southampton, UK) was applied over the closed sutured scalp. Animals were then allowed to recover in a thermostatically-controlled container before returning to individual housing with *ad libitum* food and water. Their drinking water contained paracetamol (Sterwin Medicines, UK; 500 mg/L) and sucrose (2%) after surgery. Each animal's health was monitored daily.

Wheat-germ agglutinin anterograde labelling

Animals were perfused with 4% buffered paraformaldehyde, and the brains then removed and postfixed for 4 h in paraformaldehyde and finally transferred to 30% sucrose solution in 0.1 M PBS for 24 h to cryoprotect the tissue before cutting. Brains were placed on a freezing platform and a 1-in-3 series of 40 μm coronal sections cut on a sledge microtome (Leica 1400). An antiserum directed against the WGA (Vector Laboratories) was used at a dilution of 1:2000 and incubated at 4 °C for 48 h. The antigen-antibody complex was localized with a standard avidin-biotin process (ABC Elite Kit, Vector Laboratories). The chromogen diaminobenzidine produced the visualized reaction, which was further enhanced with a nickel solution (DAB Substrate Kit, Vector Laboratories).

Wheat-germ agglutinin-horseradish peroxidase anterograde labelling

Animals were perfused with 1.5% buffered paraformaldehyde with 1% gluteraldehyde, after which the brains were removed and further postfixed for 2 h before being transferred to 30% sucrose solution in 0.1 M PBS for 24 h to cryoprotect the tissue before cutting. Brains were cut as described, with the exceptions that sections were cut at 50 μm and the second series was reacted for the presence of horseradish peroxidase (HRP) following an ammonium molybdate–tetramethylbenzidine protocol. Following both reactions, sections were then mounted onto gelatin-subbed slides and dehydrated through increasing concentrations of alcohol before being cover-slipped from xylene with DPX (Raymond Lamb, Eastbourne, UK). A Leica DM5000B microscope with a Leica DFC350FX digital camera was used to

capture images. Photoshop (Adobe Systems, Inc.) was used to enhance the sharpness and contrast of the photomicrographs.

Wheat-germ agglutinin injection into the mammillary bodies

Case SVR 39_12 used bilateral 0.02 μl injections of 2% WGA (Vector Laboratories) injected into the mammillary bodies. The injections were centred at: AP −1.9, ML ±0.8, DV −10.4 from bregma. The animal survived for 24 h after surgery to allow direct labelling of pathways and to prevent transneuronal labelling.

Wheat-germ agglutinin-horseradish peroxidase injection into the subiculum

Case SVR 40_3 used a single unilateral 0.02 μl injection of 2% WGA-HRP (Vector Laboratories) into the dorsal subiculum. The injection was centred at: AP −5.2, ML ±3.6, DV −6.4 from bregma. The rat survived for 24 h after surgery to allow only direct retrograde uptake of tracer.

Electrophysiological experiments, surgical preparation

Under urethane anesthesia (ethyl carbamate: 1.5 g/kg, i.p.), the animals underwent implantation of a monopolar recording electrode (RNEX-300, Kopf Instruments) in the anterior thalamic nuclei and bipolar stimulating electrodes in the descending hippocampal fornix (Fx) and concurrently in the mammillothalamic tract (MTT). The nose bar was positioned on a level that ensured the location of Bregma and Lambda on the same horizontal plane.

For the recording electrode, a drill hole was made (1-mm in diameter), 1.3–1.6 mm posterior to bregma and 1.4–1.6 mm lateral to the midline, corresponding to the anterior thalamic nuclei in the rat (Kruger et al., 1995). A second drill hole was made for a bipolar stimulating electrode with coordinates targeting Fx (3.3–3.5 mm posterior to bregma, 0.3–0.5 mm lateral to midline, Fig. 1B) or alternatively MTT (2.3–2.5 mm posterior to bregma, 0.8– 1.0 mm lateral to midline, Fig. 1C). The dorsoventral positioning of the electrodes was as follows: 4.5–5.5 mm from the dural surface for ATN (Fig. 1D), 1.5–2.5 mm for Fx and 5.0–6.0 mm for MTT. Final positions of the stimulating and recording electrodes were then determined by maximizing the amplitude of the field potential recorded in the ATN in response to electrical stimulation of MTT/Fx. Monopolar recordings from ATN were made relative to ground and reference screws inserted into the contralateral parietal and frontal bones. We used large-diameter (100 μm) low-impedance electrodes (50–250 kΩ). Thalamic local field potentials measured with such electrodes have been recently shown to reflect to the theta oscillatory activity of single theta cells in anterior thalamus (Tsanov et al., 2011a). Once verification of the location of the electrodes was complete, recordings were allowed to stabilize for 10 min prior to the experiment.

Measurement of local field activity

The local field potential (LFP) was sampled at 0.5 kHz and stored for further off-line analysis. In order to evaluate delta (1.5–3.0 Hz), low theta (3.0–5.5 Hz) and high theta (5.5–11 Hz) oscillatory activity during the course of experiment, 4-s long epochs 1 s after each test-pulse were selected. Fourier analysis of artefact-free epochs was performed with the Hanning window function using “Spike2” software (CED). The absolute values of spectral power for each individual animal were transformed into relative ones (with the mean value for the baseline prestimulation period taken as 100%) that were then used further for statistics. For each time-point, the results of Fourier analysis of five epochs were averaged. Theta activity was measured by the ratio between the relative values of theta and delta spectral powers (T-ratio).

Measurement of evoked field potentials

The field potential (FP) recordings were performed as previously described (Tsanov et al., 2011b). Briefly, the signals were filtered between 0.1 Hz and 1 kHz, and then amplified (DAM-50 differential amplifier; World Precision Instruments, Hertfordshire, UK). Recordings were digitized online using a PC connected to a CED-1401 plus interface and analyzed using "Spike2" software (CED, Cambridge, UK). Thalamic FPs were evoked by MTT/Fx stimulation at a low frequency (0.025 Hz). The same baseline frequency was used for the parallel Fx–MTT recordings where MTT test-pulses followed the Fx pulses with a 20 s time difference. For each time-point measured during the experiments, five records of evoked responses were averaged. The FP slope was measured as the intermediate 90% of the slope value between the first positive and the first negative deflections of the FP. The FP amplitude represents the absolute difference between the value of the first positive and the value of the first negative deflections of the FP. Baseline responses were collected for 120 min before the application of the low-frequency stimulation (LFS) protocol. The subsequent recording of ATN FPs continued for 150 min and was followed by high-frequency stimulation (HFS). LFS comprised frequency of 1 Hz (900 pulses) whereas HFS consisted of 10 bursts, with each burst containing 10 pulses at 100 Hz, with an interburst interval of 10 s.

Statistical analyses

Electrophysiological data were expressed as the mean percentage of baseline FP reading ±standard error of the mean (SEM). Statistical significance was estimated by using factorial analysis of variance (ANOVA) and post hoc Student's *t*-test and Tukey test. Using factorial ANOVA, we estimated the effects of stimulation protocol and time on the field potential values, compared to baseline. The probability level interpreted as statistically significant was $P<0.05$. For correlation analyses, we used Pearson's coefficient.

Post mortem verification of electrode site

At the end of the study, brains were removed for histological verification of electrode localization. The animals underwent transcardial perfusion with 0.1 M PBS followed by 10% formol-saline. The brains were postfixed in 10% formol-saline and then transferred to 25% sucrose overnight. Brain sections (16 μm) were stained according to the Nissl method using 1% Toluidine Blue, and then examined using a light microscope. Brains in which incorrect electrode localization was found were discarded from the study.

RESULTS

Subiculum and medial mammillary bodies provide dense projections to the anteroventral nucleus

To confirm that our stimulation electrodes target the appropriate presynaptic subicular and mammillary efferent fibers, we injected anterograde markers into the regions that give rise to fornix and mammillothalamic tract, respectively. The anterograde tracing also allowed us to locate the precise dorsoventral coordinates of thalamic neuronal population that receives fornical and MTT afferents. The immuno-detection of anterograde-labelled anteroventral cells after WGA injection in the medial mammillary bodies demonstrated robust mammillothalamic projections to anteroventral cells (Fig. 2A). Likewise, WGA-HRP injections into dorsal subiculum (corresponding to the cellular output of our electrode target) resulted in anterograde labelling within the anterior thalamic nuclei. This anterior thalamic label was most dense in anteroventral nucleus (Fig. 2B). Therefore, we confirmed that subicular and mammillary efferents comprise two major monosynaptic inputs to rat anterior thalamic nuclei. The obtained dorsoventral coordinates from the labelled anteroventral

neurons also served as a guidance for our recording electrode implantation (see Experimental procedures). For the induction of synchronous synaptic potentials in ATN, we implanted stimulation electrodes in the subicular and mammillothalamic pathways targeting ATN: the fornix and the mammillothalamic tract, respectively (Fig. 3A inset). Our aim was to demonstrate that the stimulus-evoked field activity is not a reflection of general aminergic arousal always triggered during theta episodes in freely-behaving animals. For this reason, we examined the hippocampo-diencephalic interaction of behaviorally-inactive rats under urethane anesthesia.

Theta spectral power increases after low-frequency stimulation of fornix, but not mammillothalamic tract

To examine which major input influences theta in ATN, we stimulated the descending hippocampal Fx and the ascending MTT with plasticity-inducing protocols, and recorded the LFP signal from the ipsilateral ATN. After 120 min baseline recordings with a test-pulse frequency of 0.025 Hz, the stimulation rate was set to 1 Hz for the following 900 pulses (Fig. 3B). In order to distinguish the effect of frequency parameters of the stimulation protocol, 150 min after LFS, we applied 100 Hz HFS. Our previous recordings revealed that HFS applied after baseline recordings has a smaller effect on thalamic responsiveness, compared to LFS (Tsanov et al., 2011b). For this reason, our experimental protocol started first with LFS (Fig. 3B). The lower frequency of the recorded theta oscillation (Fig. 3C, D), compared to freely-moving recordings, is a specific feature of limbic theta recorded under urethane anaesthesia (Manns et al., 2003).

LFP spectral power analysis demonstrated a dissociation between low-frequency delta and higher-frequency theta immediately after LFS protocol (Fig. 3E). This change was expressed with an augmentation of theta-power and a suppression of delta-power. This dissociation lasted for 45–60 min, but rose twice for the 150 min of post-LFS recordings. The mean values of the measured theta and delta spectral values after HFS (Fig. 3E) were not significantly different compared to the initial baseline recording period. The comparative dynamics of theta and delta can be represented as the theta ratio (T-ratio—the ratio of the relative values of theta and delta spectral powers per time bin) (Harris et al., 2002). T-ratio analyses reveal that LFS-evoked increase of T-ratio produced more robust changes in the low band of theta rhythm (3.0–5.5 Hz) (Fig. 4A, Tukey, $P<0.05$, $n=5$) and, to a lesser degree, in the higher band of 5.5–11 Hz (Fig. 4B, Tukey, $P<0.05$, $n=5$). The mean value of ATN theta activity from all animals in the group revealed a significant augmentation after LFS to fornix, compared to the pre-stimulation baseline period (Fig. 4A–D). While fornix-LFS induced opposing changes of theta and delta spectral powers, MTT-LFS resulted in a similar modification of both rhythms (Fig. 3F). We found a gradual decrease that was more expressed for delta and less expressed for theta power as a consequence of LFS. The long time-scale evaluation of theta activity through the theta/delta ratios did not reveal a prominent increase in theta oscillation after LFS. Unlike fornix-mediated T-ratio augmentation, MTT-mediated thalamic field activity was not significantly higher compared to baseline measurements (ANOVA, $F<1$, $P>0.05$, $n=5$; Fig. 4E–H).

Theta rhythm augmentation correlates only with the fornix-evoked ATN field depression

Analyses of the first 20 ms of the post-stimulus LFP signal revealed another difference between fornix- and MTT-mediated impacts on thalamic physiology. LFS of the fornix induced an immediate decrease (20–25%) in the evoked FP (Fig. 5A). Both FP slope (ANOVA, $F_{(1,49)}=3.67$, $P<0.01$, $n=5$) and FP amplitude (ANOVA, $F_{(1,49)}=4.12$, $P<0.01$, $n=5$) underwent long-term depression for 150 min. Applying LFS to the mammillothalamic tract did not induce depression (Fig. 5B); instead, we detected a significant potentiation of

FP slope, compared to baseline values measured 60 min prior to LFS (ANOVA, $F_{(1,49)}$=2.80, P<0.01, n=6).

Comparison of oscillatory and FP fluctuations for each animal throughout the fornix-stimulation experiments revealed parallel modifications after the stimulation protocols, and also for the baseline period. Both FP slope (Fig. 5C) and FP amplitude (Fig. 5D) shared the same profile. We found a significant negative correlation between FP slope and the low T-ratio (the ratio between low theta and delta; Fig. 5E, Pearson, P<0.001, r=−0.4470, n=5) as well as between FP slope and high T-ratio (the ratio between high theta and delta; Fig. 5F, Pearson, P<0.001, r=−0.3674, n=5). Similarly, FP amplitude was significantly correlated with both low (Pearson, P<0.001, r=−0.3381, n=5; data not shown) and high T-ratios (Pearson, P<0.001, r=−0.2544, n=5; data not shown). Unlike the fornix-evoked concurrency between theta and FP, MTT stimuli were not characterized by a similar time-course for the low T-ratio fluctuations and FP slope (Fig. 5G). Similarly, no concurrence was observed between low T-ratio and FP amplitude (Fig. 5H). The low T-ratio did not correlate significantly with the FP slope induced by MTT pulses (Fig. 5I, Pearson, P=0.468, r=0.0419, n=6), while the correlation of the FP slope to the high T-ratio was positive (Fig. 5J, Pearson P<0.001, r=0.2746, n=6). A similar correlation was evident between FP amplitude and high T-ratio (Pearson, P<0.001, r=0.2064, n=6; data not shown).

DISCUSSION

The data presented here provide evidence that hippocampal activity mediates concurrent changes of theta rhythm and neuronal responsiveness in anterior thalamus. We find that these changes are evoked only after the stimulation of the direct hippocampal output to ATN, but not after the stimulation of the mammillothalamic tract. Our findings support the idea that hippocampal theta modifies thalamic responsiveness to stimuli coming from the tegmental area via the mammillary bodies.

Inactivation of medial septum can abolish the theta rhythmical discharge in both hippocampus and mammillary bodies (Kirk et al., 1996) and this finding opens the question of the difference between ascending mammillothalamic and descending hippocampal efferents on the theta properties of anterior thalamus. In order to explain the functional differences of the ATN inputs, we need a clear view of how mammillothalamic and direct hippocampal projections differ in their ability to control the major feature of ATN: its theta rhythm. Using anterograde labeling, we confirmed the dense anatomical connectivity of the dorsal subiculum and medial mammillary bodies to anteroventral nucleus (Ishizuka, 2001; Wright et al., 2010). These projections reach anterior thalamus via the postcommissural fornix and mammillothalamic tract, respectively (Meibach and Siegel, 1975; Ishizuka, 2001). We compared the parallel oscillatory properties in ATN occurring after plasticity-inducing stimulation protocols to MTT and fornix under urethane anesthesia. LFS to fornix induced augmentation of thalamic low- and high-theta ratios (theta over delta) for about 120 min. In contrast, the same protocol applied to MTT failed to evoke significant oscillatory changes. HFS protocol applied to either fornix or MTT did not result in long-lasting theta effects.

Anteroventral nucleus, which was the target of our recordings, is characterized by neurons that tend to oscillate in the theta spectral band (Vertes et al., 2001). Approximately one-third of the cells in the anteroventral nucleus fire rhythmically in theta range (Tsanov et al., 2011a). Theta rhythm is believed to serve a critical role in the mnemonic functions of the limbic system (Burgess et al., 2002; Buzsáki, 2005). Previous experiments demonstrate the loss of theta with reversible or irreversible lesions of the medial septum significantly altering performance of spatial (Mizumori et al., 1990; M'Harzi and Jarrard, 1992; Leutgeb and

Mizumori, 1999) as well as nonspatial (Mizumori et al., 1990; Asaka et al., 2002) tasks in rodents. Consistent with this view, electrophysiological studies in rats have found that plasticity occurs between sequentially-activated hippocampal place cells during theta epochs (Skaggs et al., 1996; Mehta et al., 2000, 2002; Ekstrom et al., 2001), thus suggesting that the theta cycle may function as an information quantum (Buzsáki, 2002).

Synaptic depression has been proposed as a dynamic gain control mechanism in cortical information processing (Abbott et al., 1997); it has been negatively correlated with oscillatory activity in thalamocortical systems (Tsanov and Manahan-Vaughan, 2007). Furthermore, recent data demonstrate a negative correlation between hippocampal theta rhythm and exploration-induced depression of entorhino-hippocampal synaptic transmission (Tsanov and Manahan-Vaughan, 2008). Importantly, the negative correlation between theta power and the field potential observed in our ATN recordings is input-specific and relevant only to the stimulation of hippocampal output via the descending fornix projections. Similarly, fornix lesions have been shown to disrupt the spiking activity of rabbit anteroventral neurons (Smith et al., 2004). However, MTT pulses did not evoke continuous concurrent oscillatory and plastic changes in ATN. Overall, ATN spectral power revealed no correlation between FP slope and low T-ratio, and a significant positive correlation between FP parameters and high T-ratio. The observed result could be related to the physiological role of the ascending flow of Papez's circuit to mediate motion-dependent theta, in which values fall within a range of 8–12 Hz (high theta) (Bland et al., 1984; Bland, 1986; Sainsbury et al., 1987).

Thalamus and cortex are considered as a loop that dynamically regulates signal processing (Ergenzinger et al., 1998; Parker and Dostrovsky, 1999). Concordantly, the patterns of episodic memory loss seen in patients with anterior thalamic pathology are similar to those seen in patients with lesions in the medial temporal lobe (Harding et al., 2000; Van der Werf et al., 2000). Furthermore, restricted pathologies from tumors and traumatic injury also reveal the contributions of the mammillary bodies to episodic memory (Dusoir et al., 1990; Tsivilis et al., 2008). Importantly, animal models using localized lesions reveal that mammillary bodies or MTT lesion impairments has less severe effects on spatial memory tasks than those following ATN lesions, the latter being often comparable to fornix lesions (Aggleton et al., 1991, 1995, but also see Vann and Albasser, 2009). The above-mentioned clinical findings and lesion studies strongly suggest that the anterior thalamus functionally complements the hippocampal region for memory processing (Aggleton et al., 2010). Our data, which reveal the theta-mediated relationship between these regions, support this view.

CONCLUSION

In conclusion, our data show that low-frequency stimulation augments the amplitude of thalamic theta spectral power selectively when applied to dorsal fornix. The same protocol fails to increase theta in anterior thalamus when applied to the mammillothalamic tract. We also demonstrate that low-frequency stimulation evokes, in parallel, depression of thalamic synaptic responses. In comparison, thalamic field potential did not correlate with local theta power after low-frequency stimulation of mammillothalamic tract. Thus, we conclude that the descending fornix is a pathway that dynamically modulates the oscillatory properties of anterior thalamus.

Acknowledgments

This work was supported by a Wellcome Trust grant #081075 to John P. Aggleton, Shane M. O'Mara, Jonathan T. Erichsen and Seralynne D. Vann.

Abbreviations

ANOVA	analysis of variance
ATN	anterior thalamic nuclei
FP	field potential
Fx	fornix
HFS	high-frequency stimulation
LFP	local field potential
LFS	low-frequency stimulation
MTT	mammillothalamic tract
WGA	wheat germ agglutinin
WGA-HRP	wheat germ agglutinin conjugated to horseradish peroxidase

REFERENCES

Abbott LF, Varela JA, Sen K, Nelson SB. Synaptic depression and cortical gain control. Science. 1997; 275:220–224. [PubMed: 8985017]

Aggleton JP, Keith AB, Sahgal A. Both fornix and anterior thalamic, but not mammillary, lesions disrupt delayed non-matching-to-position memory in rats. Behav Brain Res. 1991; 44:151–161. [PubMed: 1751006]

Aggleton JP, Neave N, Nagle S, Hunt PR. A comparison of the effects of anterior thalamic, mamillary body and fornix lesions on reinforced spatial alternation. Behav Brain Res. 1995; 68:91–101. [PubMed: 7619309]

Aggleton JP, O'Mara SM, Vann SD, Wright NF, Tsanov M, Erichsen JT. Hippocampal-anterior thalamic pathways for memory: uncovering a network of direct and indirect actions. Eur J Neurosci. 2010; 31:2292–2307. [PubMed: 20550571]

Aggleton JP, Sahgal A. The contribution of the anterior thalamic nuclei to anterograde amnesia. Neuropsychologia. 1993; 31:1001–1019. [PubMed: 8290019]

Alonso A, Llinas RR. Subthreshold Na+-dependent theta-like rhythmicity in stellate cells of entorhinal cortex layer II. Nature. 1989; 342:175–177. [PubMed: 2812013]

Asaka Y, Griffin AL, Berry SD. Reversible septal inactivation disrupts hippocampal slow-wave and unit activity and impairs trace conditioning in rabbits (*Oryctolagus cuniculus*). Behav Neurosci. 2002; 116:434–442. [PubMed: 12049324]

Bland BH. The physiology and pharmacology of hippocampal formation theta rhythms. Prog Neurobiol. 1986; 26:1–54. [PubMed: 2870537]

Bland BH, Seto MG, Sinclair BR, Fraser SM. The pharmacology of hippocampal theta cells: evidence that the sensory processing correlate is cholinergic. Brain Res. 1984; 299:121–131. [PubMed: 6326959]

Brazhnik ES, Vinogradova OS. Control of the neuronal rhythmic bursts in the septal pacemaker of theta-rhythm: effects of anaesthetic and anticholinergic drugs. Brain Res. 1986; 380:94–106. [PubMed: 3756475]

Burgess N, Maguire EA, O'Keefe J. The human hippocampus and spatial and episodic memory. Neuron. 2002; 35:625–641. [PubMed: 12194864]

Buzsáki G. Theta oscillations in the hippocampus. Neuron. 2002; 33:325–340. [PubMed: 11832222]

Buzsáki G. Theta rhythm of navigation: link between path integration and landmark navigation, episodic and semantic memory. Hippocampus. 2005; 15:827–840. [PubMed: 16149082]

Dragoi G, Harris KD, Buzsáki G. Place representation within hippocampal networks is modified by long-term potentiation. Neuron. 2003; 39:843–853. [PubMed: 12948450]

Dusoir H, Kapur N, Byrnes DP, McKinstry S, Hoare RD. The role of diencephalic pathology in human memory disorder. Evidence from a penetrating paranasal brain injury. Brain. 1990; 113(Pt 6): 1695–1706. [PubMed: 2276041]

Ekstrom AD, Meltzer J, McNaughton BL, Barnes CA. NMDA receptor antagonism blocks experience-dependent expansion of hippocampal “place fields.”. Neuron. 2001; 31:631–638. [PubMed: 11545721]

Ergenzinger ER, Glasier MM, Hahm JO, Pons TP. Cortically induced thalamic plasticity in the primate somatosensory system. Nat Neurosci. 1998; 1:226–229. [PubMed: 10195147]

Fortin NJ, Agster KL, Eichenbaum HB. Critical role of the hippocampus in memory for sequences of events. Nat Neurosci. 2002; 5:458–462. [PubMed: 11976705]

Gold JJ, Squire LR. The anatomy of amnesia: neurohistological analysis of three new cases. Learn Mem. 2006; 13:699–710. [PubMed: 17101872]

Harding A, Halliday G, Caine D, Kril J. Degeneration of anterior thalamic nuclei differentiates alcoholics with amnesia. Brain. 2000; 123(Pt 1):141–154. [PubMed: 10611128]

Harris KD, Henze DA, Hirase H, Leinekugel X, Dragoi G, Czurko A, Buzsáki G. Spike train dynamics predicts theta-related phase precession in hippocampal pyramidal cells. Nature. 2002; 417:738–741. [PubMed: 12066184]

Hasselmo ME. What is the function of hippocampal theta rhythm?—linking behavioral data to phasic properties of field potential and unit recording data. Hippocampus. 2005; 15:936–949. [PubMed: 16158423]

Henry J, Petrides M, St-Laurent M, Sziklas V. Spatial conditional associative learning: effects of thalamo-hippocampal disconnection in rats. Neuroreport. 2004; 15:2427–2431. [PubMed: 15640769]

Hoffmann LC, Berry SD. Cerebellar theta oscillations are synchronized during hippocampal theta-contingent trace conditioning. Proc Natl Acad Sci U S A. 2009; 106:21371–21376. [PubMed: 19940240]

Hyman JM, Wyble BP, Goyal V, Rossi CA, Hasselmo ME. Stimulation in hippocampal region CA1 in behaving rats yields long-term potentiation when delivered to the peak of theta and long-term depression when delivered to the trough. J Neurosci. 2003; 23:11725–11731. [PubMed: 14684874]

Ishizuka N. Laminar organization of the pyramidal cell layer of the subiculum in the rat. J Comp Neurol. 2001; 435:89–110. [PubMed: 11370013]

Kirk IJ, Oddie SD, Konopacki J, Bland BH. Evidence for differential control of posterior hypothalamic, supramammillary, and medial mammillary theta-related cellular discharge by ascending and descending pathways. J Neurosci. 1996; 16:5547–5554. [PubMed: 8757266]

Kruger, L.; Saporta, S.; Swanson, LW. Photographic atlas of the rat brain: the cell and fiber architecture illustrated in three planes with stereotaxic coordinates. Cambridge University Press; New York: 1995.

Leung LW, Yim CY. Intrinsic membrane potential oscillations in hippocampal neurons *in vitro*. Brain Res. 1991; 553:261–274. [PubMed: 1718544]

Leutgeb S, Mizumori SJ. Excitotoxic septal lesions result in spatial memory deficits and altered flexibility of hippocampal single-unit representations. J Neurosci. 1999; 19:6661–6672. [PubMed: 10414995]

Linden DJ. The return of the spike, postsynaptic action potentials and the induction of LTP and LTD. Neuron. 1999; 22:661–666. [PubMed: 10230787]

M’Harzi M, Jarrard LE. Effects of medial and lateral septal lesions on acquisition of a place and cue radial maze task. Behav Brain Res. 1992; 49:159–165. [PubMed: 1388809]

Manns ID, Alonso A, Jones BE. Rhythmically discharging basal forebrain units comprise cholinergic, GABAergic, and putative glutamatergic cells. J Neurophysiol. 2003; 89:1057–1066. [PubMed: 12574480]

Mehta MR, Lee AK, Wilson MA. Role of experience and oscillations in transforming a rate code into a temporal code. Nature. 2002; 417:741–746. [PubMed: 12066185]

Mehta MR, Quirk MC, Wilson MA. Experience-dependent asymmetric shape of hippocampal receptive fields. Neuron. 2000; 25:707–715. [PubMed: 10774737]

Meibach RC, Siegel A. The origin of fornix fibers which project to the mammillary bodies in the rat: a horseradish peroxidase study. Brain Res. 1975; 88:508–512. [PubMed: 49209]

Mizumori SJ, Perez GM, Alvarado MC, Barnes CA, McNaughton BL. Reversible inactivation of the medial septum differentially affects two forms of learning in rats. Brain Res. 1990; 528:12–20. [PubMed: 2245328]

Parker A, Gaffan D. The effect of anterior thalamic and cingulate cortex lesions on object-in-place memory in monkeys. Neuropsychologia. 1997; 35:1093–1102. [PubMed: 9256374]

Parker JL, Dostrovsky JO. Cortical involvement in the induction, but not expression, of thalamic plasticity. J Neurosci. 1999; 19:8623–8629. [PubMed: 10493762]

Sainsbury RS, Harris JL, Rowland GL. Sensitization and hippocampal type 2 theta in the rat. Physiol Behav. 1987; 41:489–493. [PubMed: 3432404]

Seidenbecher T, Laxmi TR, Stork O, Pape HC. Amygdalar and hippocampal theta rhythm synchronization during fear memory retrieval. Science. 2003; 301:846–850. [PubMed: 12907806]

Skaggs WE, McNaughton BL, Wilson MA, Barnes CA. Theta phase precession in hippocampal neuronal populations and the compression of temporal sequences. Hippocampus. 1996; 6:149–172. [PubMed: 8797016]

Smith DM, Wakeman D, Patel J, Gabriel M. Fornix lesions impair context-related cingulothalamic neuronal patterns and concurrent discrimination learning in rabbits (*Oryctolagus cuniculus*). Behav Neurosci. 2004; 118:1225–1239. [PubMed: 15598132]

Steriade M. Impact of network activities on neuronal properties in corticothalamic systems. J Neurophysiol. 2001; 86:1–39. [PubMed: 11431485]

Tsanov M, Chah E, Wright N, Vann SD, Reilly R, Erichsen JT, Aggleton JP, O'Mara SM. Oscillatory entrainment of thalamic neurons by theta rhythm in freely moving rats. J Neurophysiol. 2011a; 105:4–17. [PubMed: 20962067]

Tsanov M, Manahan-Vaughan D. Intrinsic, light-independent and visual activity-dependent mechanisms cooperate in the shaping of the field response in rat visual cortex. J Neurosci. 2007; 27:8422–8429. [PubMed: 17670989]

Tsanov M, Manahan-Vaughan D. Synaptic plasticity from visual cortex to hippocampus: systems integration in spatial information processing. Neuroscientist. 2008; 14:584–597. [PubMed: 18612086]

Tsanov M, Manahan-Vaughan D. Visual cortex plasticity evokes excitatory alterations in the hippocampus. Front J Integr Neurosci. 2009; 3:32. [PubMed: 19956399]

Tsanov M, Vann SD, Erichsen JT, Wright N, Aggleton JP, O'Mara SM. Differential regulation of synaptic plasticity of the hippocampal and the hypothalamic inputs to the anterior thalamus. Hippocampus. 2011b; 21:1–8. [PubMed: 20043283]

Tsivilis D, Vann SD, Denby C, Roberts N, Mayes AR, Montaldi D, Aggleton JP. A disproportionate role for the fornix and mammillary bodies in recall versus recognition memory. Nat Neurosci. 2008; 11:834–842. [PubMed: 18552840]

Van der Werf YD, Witter MP, Uylings HB, Jolles J. Neuropsychology of infarctions in the thalamus: a review. Neuropsychologia. 2000; 38:613–627. [PubMed: 10689038]

Vann SD, Aggleton JP. The mammillary bodies: two memory systems in one? Nat Rev Neurosci. 2004; 5:35–44. [PubMed: 14708002]

Vann SD, Albasser MM. Hippocampal, retrosplenial, and pre-frontal hypoactivity in a model of diencephalic amnesia: evidence towards an interdependent subcortical-cortical memory network. Hippocampus. 2009; 19:1090–1102. [PubMed: 19280662]

Vertes RP, Albo Z, Viana Di Prisco G. Theta-rhythmically firing neurons in the anterior thalamus: implications for mnemonic functions of Papez's circuit. Neuroscience. 2001; 104:619–625. [PubMed: 11440795]

Warburton EC, Baird A, Morgan A, Muir JL, Aggleton JP. The conjoint importance of the hippocampus and anterior thalamic nuclei for allocentric spatial learning: evidence from a disconnection study in the rat. J Neurosci. 2001; 21:7323–7330. [PubMed: 11549742]

Warburton EC, Baird AL, Morgan A, Muir JL, Aggleton JP. Disconnecting hippocampal projections to the anterior thalamus produces deficits on tests of spatial memory in rats. Eur J Neurosci. 2000; 12:1714–1726. [PubMed: 10792449]

Wikgren J, Nokia MS, Penttonen M. Hippocampo-cerebellar theta band phase synchrony in rabbits. Neuroscience. 2010; 165:1538–1545. [PubMed: 19945512]

Wolff M, Gibb SJ, Dalrymple-Alford JC. Beyond spatial memory: the anterior thalamus and memory for the temporal order of a sequence of odor cues. J Neurosci. 2006; 26:2907–2913. [PubMed: 16540567]

Wright NF, Erichsen JT, Vann SD, O'Mara SM, Aggleton JP. Parallel but separate inputs from limbic cortices to the mammillary bodies and anterior thalamic nuclei in the rat. J Comp Neurol. 2010; 518:2334–2354. [PubMed: 20437531]

Ylinen A, Soltesz I, Bragin A, Penttonen M, Sik A, Buzsaki G. Intracellular correlates of hippocampal theta rhythm in identified pyramidal cells, granule cells, and basket cells. Hippocampus. 1995; 5:78–90. [PubMed: 7787949]

Europe PMC Funders Author Manuscripts

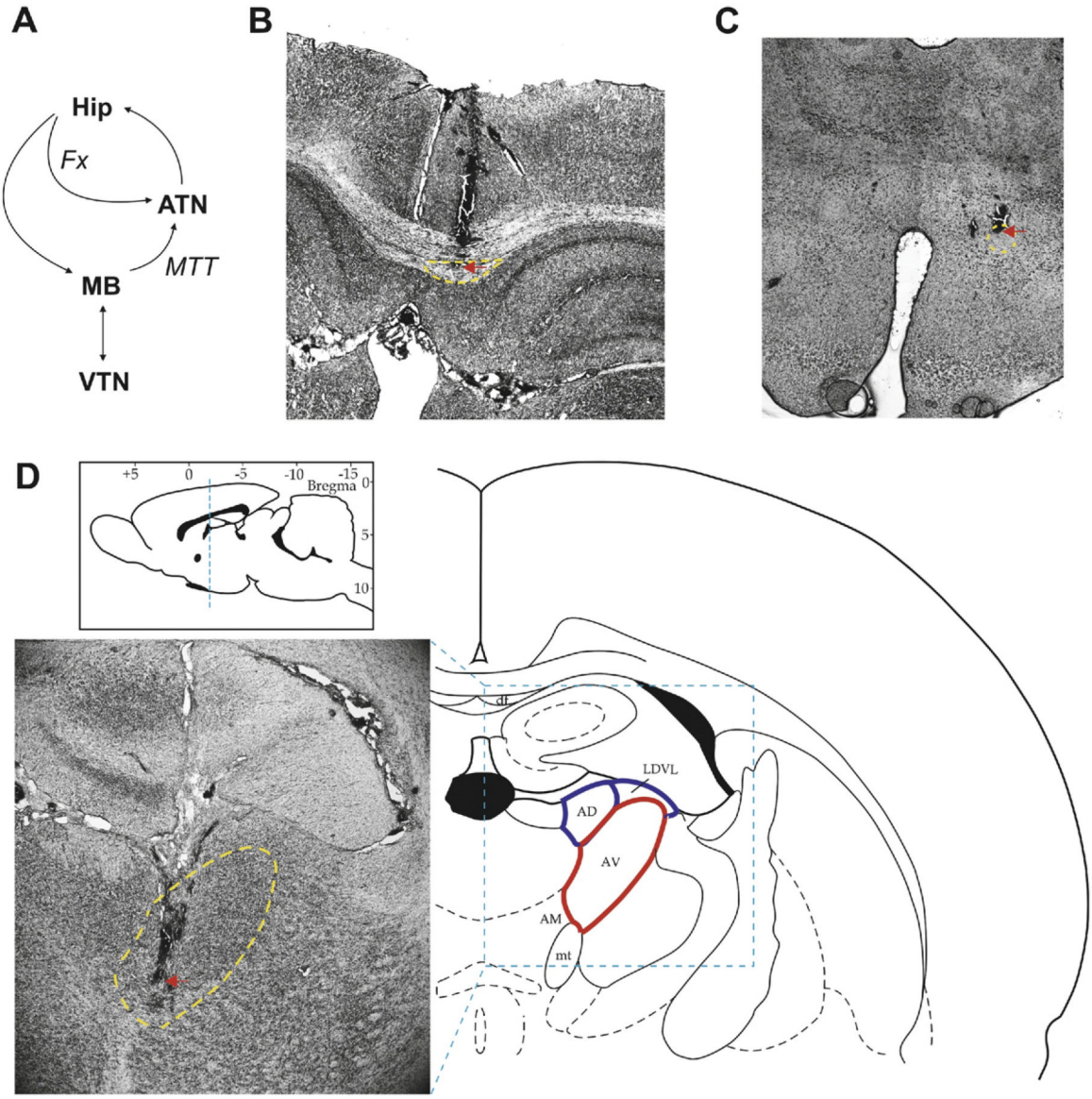

Fig. 1.

Localization of the recorded thalamic signal. (A) Hippocampo-diencephalic theta regions and their connectivity in the rodent brain. Rhythmic neuronal activity is a characteristic feature of hippocampal formation (Hip), which projects to mammillary bodies (MB) and to anterior thalamic nuclei (ATN) via the fornix (Fx). Ascending theta signal from ventral tegmental nucleus (VTN) interacts with mammillary bodies, which in turn project to ATN via mammillothalamic tract (MTT). The loop is closed by the thalamic projections to the retrosplenial cortex. To simplify the hippocampo-diencephalic theta schematic the projections from medial septum are not shown. (B) Coronal brain section showing the positioning of the stimulation electrode tip (marked with red arrow) in fornix (highlighted with yellow dashed line). (C) Coronal brain section showing the positioning of the stimulation electrode tip (marked with red arrow) in mammillothalamic tract (highlighted with yellow dashed line). (D) Coronal brain section from a rat where a recording electrode was implanted within the anteroventral nucleus of thalamus (highlighted with yellow dashed

Europe PMC Funders Author Manuscripts

line). The red arrow indicates the depth of the electrode tip. The histological section is in the coronal plane with anterior–posterior coordinates of −1.6±0.2 mm from Bregma (upper inset). The histological image is compared with rat atlas scheme (right), where anteroventral nucleus (AV, marked with red) is located ventrally from anterodorsal (AD) and laterodorsal thalamic nucleus, ventrolateral part (LDVL) (both nuclei marked with blue). For interpretation of the references to color in this figure legend, the reader is referred to the Web version of this article.

Europe PMC Funders Author Manuscripts

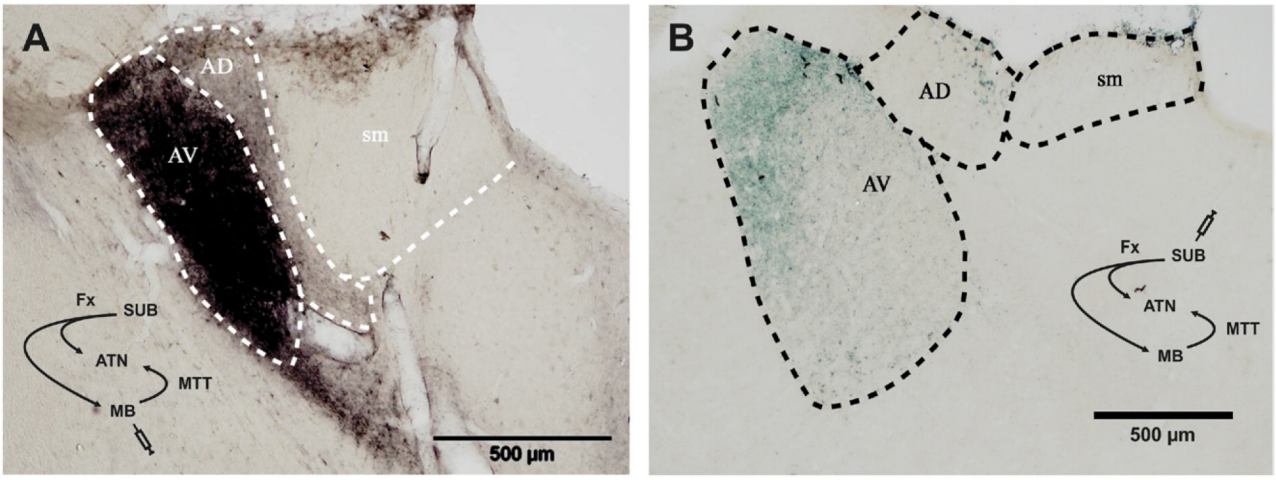

Fig. 2.

Major monosynaptic inputs to anteroventral thalamic nucleus. (A) Anterograde labelling of anteroventral nucleus (AV) after injection of wheat germ agglutinin (WGA) to medial mammillary body. The inset left-below represents the injection site within hippocampo-diencephalic circuit (Fx, fornix; MB, mammillary bodies; ATN, anterior thalamic nuclei; MTT, mammillothalamic tract). (B) Anterograde labelling of anteroventral nucleus (AV) after injection of wheat germ agglutinin conjugated to horseradish peroxidase (WGA-HRP) to dorsal subiculum (SUB). For interpretation of the references to color in this figure legend, the reader is referred to the Web version of this article.

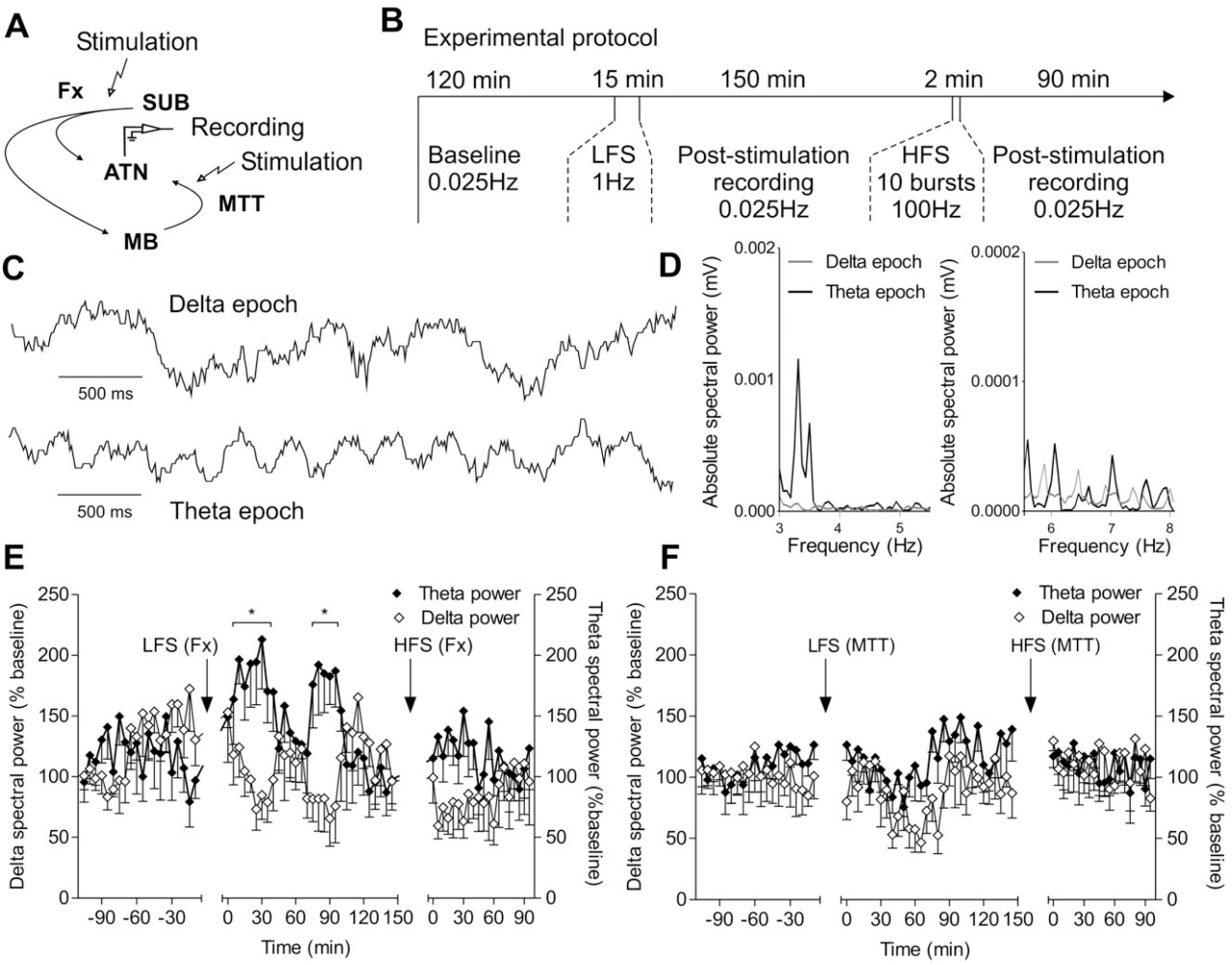

Fig. 3.

Low-frequency stimulation of fornix increases thalamic theta power. (A) Experimental design. The present experimental approach allows measurement of local field changes in the anterior thalamic nuclei (ATN) evoked after the stimulation of the two major thalamic inputs: the mammillothalamic tract (MTT), starting from mammillary bodies (MB) and the fornix (Fx) that projects directly via subicular (SUB) fibers to anterior thalamus. (B) Diagram of the experimental protocol: 120 min of baseline recording with test-pulses frequency of 0.025 Hz are followed by LFS. The subsequent post-stimulation recording lasted for 150 min; HFS preceded the second post-stimulation period of 90 min. (C) Sample delta- (upper trace) and theta LFP epoch (bottom trace). (D) Absolute spectral power ranges of low theta (3.0–5.5 Hz, left graph) and high theta (5.5–11 Hz, right graph) from AV of rats under urethane anaesthesia. Delta epoch: gray trace; theta epoch: black trace. Spectral power analyses for fornix-stimulated group (E) and MTT-stimulated group (F) following LFS and subsequent HFS. Delta power (white symbols); low theta power (black symbols). * $P<0.05$.

Europe PMC Funders Author Manuscripts

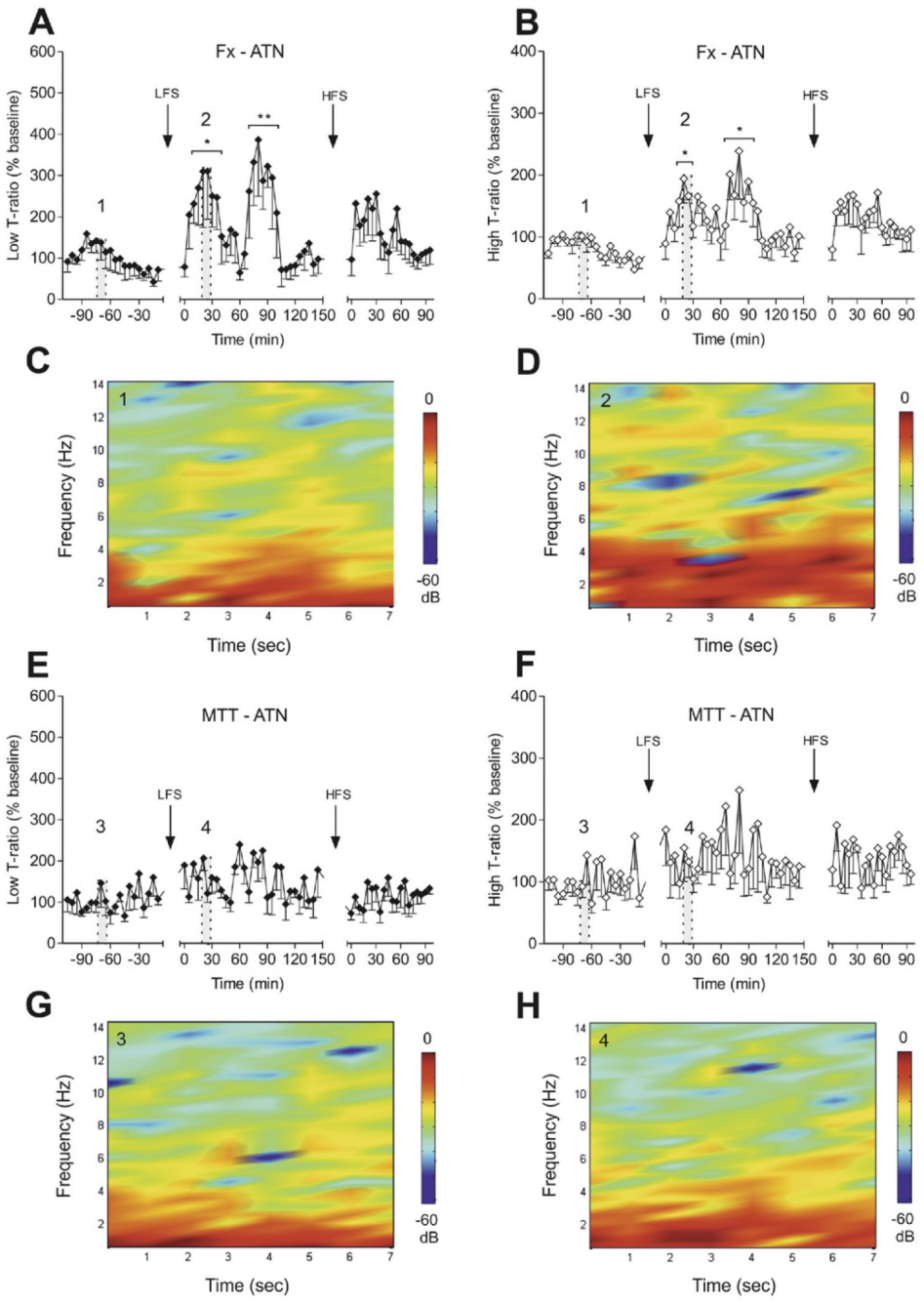

Fig. 4.

Theta ratio increases significantly after Fx, but not MTT stimulation. Low T-ratio (A) and high T-ratio (B) values following fornix-mediated LFS and subsequent HFS. * $P<0.05$, ** $P<0.01$. The numbers above the symbols denote the timing of LFP epochs on the color-coded power spectrograms below: (1) a sample epoch of the power spectrum during the baseline recording period (C), while (2) a sample epoch of the power spectrum during the subsequent post-LFS period (D). Note power increases in the 3.5–4.5 Hz range. Low T-ratio (E) and high T-ratio (F) values following MTT-mediated LFS and subsequent HFS. The numbers above the symbols denote timing of LFP epochs on the color-coded power spectrograms below: (3) represents an example epoch of the power spectrum during baseline

period (G), whereas (4) shows an example epoch of the power spectrum during the subsequent post-LFS period (H). For interpretation of the references to color in this figure legend, the reader is referred to the Web version of this article.

Europe PMC Funders Author Manuscripts

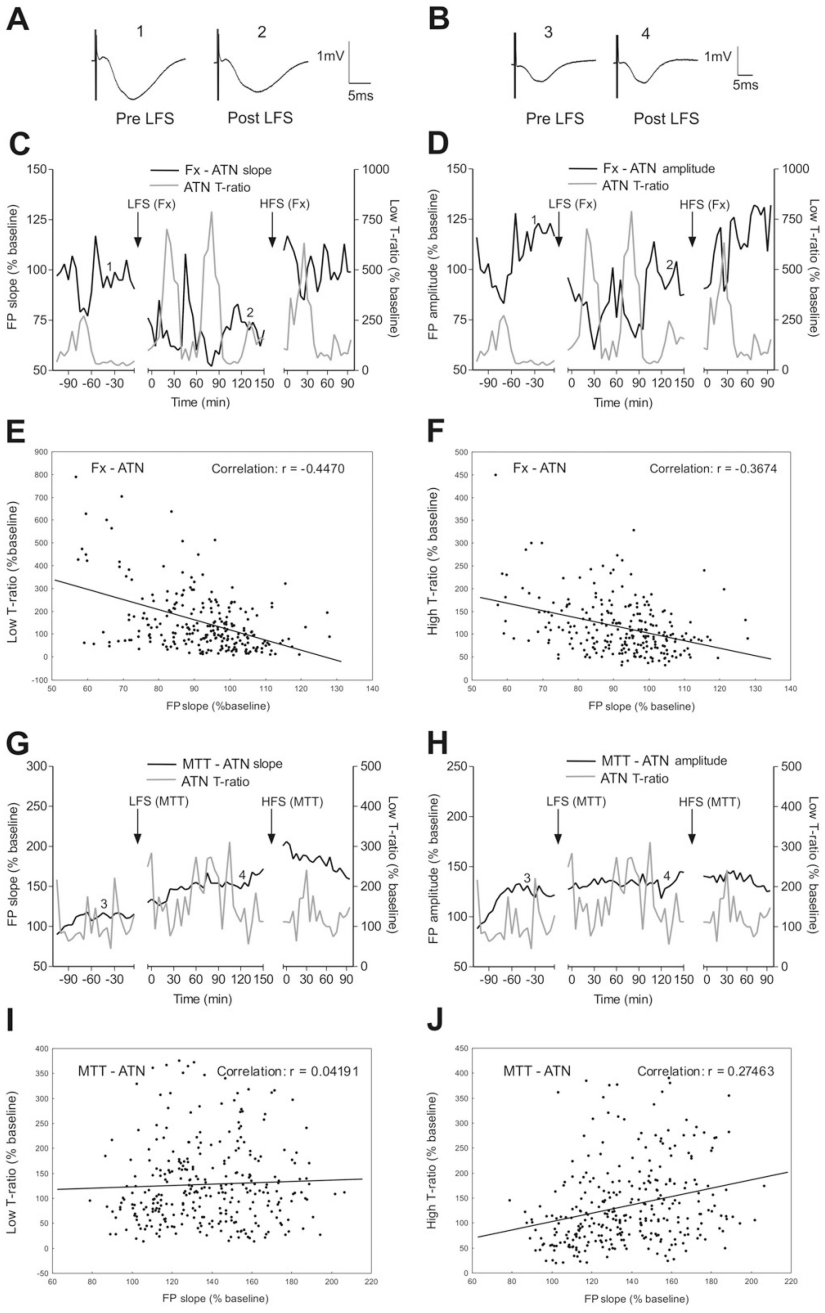

Fig. 5.

Theta ratio correlates negatively with thalamic FP parameters only after Dfx stimulation. (A) Analog traces represent field potentials (FPs) evoked before and after LFS to fornix. Horizontal bar: 5 ms, vertical bar 1 mV. The numbers above the traces refer to the exact time point denoted in (C) and (D). (B) Analog traces represent FPs evoked before and after LFS to mamillothalamic tract. Horizontal bar: 5 ms, vertical bar 1 mV. The numbers above the traces refer to the time-points denoted in (G) and (H). (C) Example of theta ratio (T-ratio; the relative values of theta-over delta-spectral powers) (grey trace) and FP slope (black trace) concurrent alterations from the group of fornix-stimulated animals. The most robust dissociation is observed after LFS, and is less prominent after HFS. (D) Similar time course

changes are evident for FP amplitude (black trace), compared to T-ratio (grey trace). (E) When averaged for all animals of the fornix-stimulated group, the analyses reveal a significant negative correlation (Pearson, $P<0.001$, $r=-0.4470$) between FP slope and low T-ratio (the ratio between low theta and delta). (F) The observed phenomenon is not restricted to the low T-ratio but is also relevant to the high T-ratio (the ratio between high theta, 5.5–11 Hz, and delta) when correlated with the FP slope (Pearson, $P<0.001$, $r=-0.3674$). (G) Example showing low T-ratio (grey trace) and FP slope (black trace) alterations from the group of MTT-stimulated animals. The T-ratio augmentation, observed mostly after LFS, has a highly fluctuating profile whereas the increase of FP slope is stable and persistent. (H) Similar time course changes are evident for the low T-ratio (grey trace) when compared to the FP amplitude (black trace). (I) Analyses of the data from the same MTT-stimulated group reveal no correlation (Pearson, $P>0.01$, $r=0.0419$) between the FP slope and the low T-ratio. (J) The high T-ratio reveals a positive correlation with the FP slope (Pearson, $P<0.01$, $r=0.2746$).

Europe PMC Funders Author Manuscripts